Melting dynamics of $NiSi_2$/Si under pulsed laser irradiation

M. G. Grimaldi, F. Priolo, P. Baeri, and E. Rimini
Dipartimento di Fisica dell'Università, Corso Italia 57, I-95129 Catania, Italy
(Received 7 August 1986; revised manuscript received 27 October 1986)

Thermally grown $NiSi_2$ layers 220 nm thick on ⟨111⟩ Si substrates have been irradiated by 40-ns Nd laser pulses with energy densities in the range 0.3—2.1 J/cm^2. Time-resolved reflectivity measurements using a He-Ne laser probe have been performed during the irradiations. Samples have been subsequently analyzed by 2.0-MeV He^+ Rutherford backscattering spectrometry in combination with the channeling effect. Three different energy-density thresholds for three phenomena have been found. At 0.37 J/cm^2 the sharp increase detected in the reflectivity signal indicates the melting of the $NiSi_2$ surface layer, at 0.92 J/cm^2 channeling measurements show the transition in the silicide layer from the $(A+B)$-type crystalline mixture to a mainly B-type single-crystal structure, and finally at 1.1 J/cm^2 the underlying silicon starts to mix with the silicide layer, modifying its stoichiometry. This behavior is discussed in terms of the phase transitions predicted from the Ni-Si phase diagram, and quantitatively is compared with kinetic calculations and the heat-flow model. Melting starts at the $NiSi_2$ free surface at $T_0=1276$ K and propagates toward the inside, while the silicon atoms at the $NiSi_2$/Si interface dissolve into the liquid solution at the $NiSi_2$ liquidus temperature (1400 K), much lower than the pure Si melting point (1685 K).

I. INTRODUCTION

Pulsed laser, ion- or electron-beam irradiation has been extensively used to induce phase transitions in surface layers. Pulses with durations of tens of nanoseconds and energy densities of about 1 J/cm^2 produce fast heating (about 10^{11} K/s) in the surface region. For suitable energy-density values, melting occurs and very fast solidification rates are subsequently achieved during cooling. Liquid-solid interface velocities of the order of several meters per second have been measured in pure silicon.[1] Under these conditions the heated system may bypass equilibrium thermodynamics rules and undergo transformations which are kinetically more favorable. For instance, the amorphous-to-liquid transition of pure silicon occurs in the nanosecond time scale[2] overcoming the amorphous-to-crystalline transition and giving rise to the existence of an undercooled liquid Si. The liquid-to-amorphous silicon transition obtained in the fast cooling regime[3] is another example in which a stable phase, i.e., the crystalline one, is suppressed by the fast kinetics. Much work has been done to understand the behavior of dilute solutions, mainly in Si-based systems, under fast heating and cooling conditions, and several phenomena like solute trapping,[4] surface segregation[5] and cellular structure[5] formation have been explained in terms of nonequilibrium thermodynamics.

Extended investigations have also been performed on the nondilute binary systems. In this case a variety of situations can be realized depending on the phase diagram of the two elements (completely miscible systems, compound-forming systems, simple eutectic systems, and so on) and on the structure of the irradiated sample (thin film on a substrate, multilayered structures, co-deposited, elements and so on). Under conditions of low concentration gradients, glassy phases have been quenched,[6] whereas large concentration gradients produce instabilities of the liquid-solid interface.[6]

Laser irradiation of metal films[7–9] on top of Si results in mixing between the two elements and in the formation of a number of different compounds. Pulsed ion-beam irradiation of Ni, Co, and Pt on Si have shown interfacial mixing at near-eutectic composition.[10] Reactions occurred below the melting temperature of either the metal or the silicon, probably at the lowest eutectic temperature. Moreover interfacial melting at the eutectic temperature has been directly detected by time-resolved temperature measurements using thin-film thermocouples in laser-irradiated Ni on Si.[11]

However modelling the metal-Si systems behavior under ultrafast heating is very complicated because one has to take into account atomic diffusion in the molten layers, heat of mixing and nucleation of new phases with completely different thermodynamic properties than the starting ones. The actual role played by equilibrium thermodynamics during the pulsed irradiation is also not quite clear. To clarify this point it is then necessary to study systems whose behavior is easily predictable by thermodynamics. Large compositional gradients in the melt must be avoided and layers with well established thermophysical properties must be used.

In the present investigation we irradiated a $NiSi_2$ layer thermally grown on monocrystalline Si substrate with Nd laser pulses. The use of this system avoids any diffusion until the substrate starts to take part in the reaction. Moreover the knowledge of the optical and thermodynamic parameters of the $NiSi_2$ allows modelling based on heat-flow calculations. The main difference between the Ni-Si and the $NiSi_2$-Si systems is the existence of a number of different compounds and eutectic compositions in

 ©1987 The American Physical Society

the phase diagram between the pure Ni and the pure Si, whilst no intermediate phases or eutectics are present between the $NiSi_2$ and the pure Si. We can then study the melting of a compound and its interaction with the underlying pure Si.

II. EXPERIMENTAL

Nickel films, 60 nm thick, were *e*-beam deposited onto chemically cleaned ⟨111⟩ oriented silicon wafers. The pressure during deposition was 10^{-7} Torr. The samples were than annealed at 400 °C for 30 min and at 800 °C for 30 min in a vacuum furnace at a pressure of 10^{-6} Torr to obtain a 220-nm-thick layer of uniform composition $NiSi_2$ on top of the silicon substrate.

Analysis of the samples was performed by Rutherford backscattering spectrometry (RBS) in combination with the channeling effect using a 2.0-MeV He^+ beam. The $NiSi_2$ film was a mixture of *A*-type crystals (epitaxial with the substrate) and *B*-type crystals (rotated 180° around the ⟨111⟩ substrate direction) in nearly equal amounts as detected by channeling analysis along the ⟨110⟩ and the ⟨114⟩ substrate directions and in agreement with previous work on the same subject.[12]

The samples were then irradiated with a 40-ns pulsed *Q*-switched Nd glass laser ($\lambda = 1.06\ \mu m$). The laser intensity was laterally homogenized within a few percent in a circular spot 3.5-mm diam by a conical light guide with a ground entrance surface. A 5-mW polarized He-Ne laser beam was focused (250-μm diam) in the center of the Nd laser spot in order to perform *in situ* time-resolved reflectivity measurements. This technique detects the occurence of surface melting due to the change in reflectivity between solid and liquid phase. The reflected beam was monitorized by a fast photodiode coupled with a storage oscilloscope and with a time resolution better than 10 ns. The polarization plane of the He-Ne laser was parallel to the incidence plane and the incidence angle was 60°. This configuration enhances the reflectivity difference between solid and liquid material.

III. RESULTS

The time-resolved reflectivity signals of our samples are reported in Fig. 1 for laser irradiations at 0.4, 0.8, and 1.0 J/cm^2. In the upper part of the same figure the temporal output of the laser pulse is shown for comparison. During the laser pulse the reflectivity signals sharply rise to a value about twice the starting value, thus indicating melting of the sample surface. The melt lasts 50, 110, and 230 ns for 0.4, 0.8, and 1.0 J/cm^2 irradiations, respectively. The surface reflectivity value after solidification stabilizes to a value 20% higher than the initial value about one microsecond after the laser pulse. This steady-state value is independent of the melt duration and can be correlated to a smoother and/or cleaner $NiSi_2$ surface after solidification compared with the thermally grown one.

The surface melt duration versus the energy density of the laser pulse is plotted in Fig. 2. The dots are values obtained from time-resolved reflectivity signals. The continuous line is a calculated trend using heat flow computer simulation which will be discussed later. The measured threshold for surface melting is 0.37 ± 0.02 J/cm^2. The error is determined by our laser energy control.

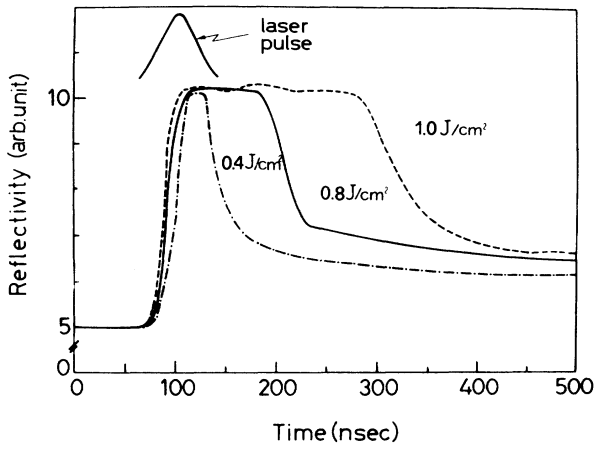

FIG. 1. Time-resolved reflectivity signals (arbitrary units) probed at the He-Ne wavelength for Nd laser irradiations of $NiSi_2$ layers at 0.4 J/cm^2 (—·—·—·), 0.8 J/cm^2 (——) and 1.0 J/cm^2 (— — —). The laser pulse is shown in the upper part.

Information on the sample structure after laser irradiation is provided by 2.0 MeV He^+ RBS analysis in combination with channeling technique. Standard channeling analysis along ⟨110⟩ and ⟨114⟩ Si substrate directions were performed to determine whether the $NiSi_2$ layer is $A+B$ type or prevalently *B* type. As stated earlier, a thermally grown $NiSi_2$ layer on ⟨111⟩ Si is a mixture of *A*- and *B*-type crystals. The $NiSi_2$ layer resulting from the liquid phase epitaxy on ⟨111⟩ Si substrate induced by the laser pulse is instead prevalently *B* type.[13] The ($A+B$)-to-*B*—type transition is then a marker for the

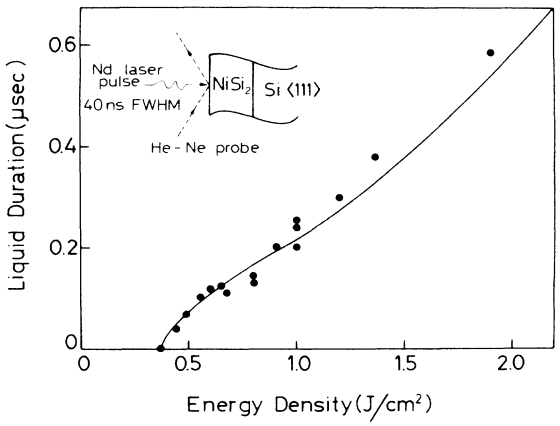

FIG. 2. Surface melt duration vs energy density. Dots refer to experimental data obtained by time-resolved reflectivity measurements. The continuous line is calculated solving the heat-flow equation.

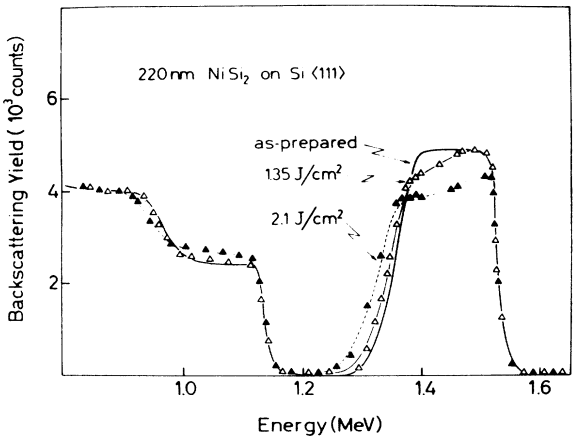

FIG. 3. 2.0 MeV He^+ Rutherford backscattering (RBS) energy spectra at random incidence for 220-nm-thick $NiSi_2$ layer on ⟨111⟩ Si before laser irradiation (solid line), after 1.35 J/cm^2 (△), and 2.1 J/cm^2 (▲) Nd pulse irradiations.

melting of the whole silicide layer. Our analysis showed the presence of a mixture of A- and B-type crystallites in all the irradiated samples up to an energy density of 0.89 J/cm^2, whilst B-type single crystals are present at irradiation above 0.95 J/cm^2.

Random spectra for the as-prepared (continuous line) sample and after subsequent irradiation with 1.35 (△) and 2.1 (▲) J/cm^2 are shown in Fig. 3. After 1.35 J/cm^2 irradiation a shift in the low energy edge associated with a decrease in the height of the Ni signal is observed. This indicates the mixing of the silicide layer with the underlying silicon in the interface region. After 2.1 J/cm^2 the mixing extends up to the silicide surface and an average composition of $Ni_{0.28}Si_{0.72}$ is measured.

Structural information obtained by channeling and backscattering analysis are summarized in Fig. 4 where the energy width of the Ni signal is plotted as a function of the laser pulse energy density. The open and closed dots refer to samples in which the silicide layer is ($A+B$)-type and mainly B-type, respectively. Taking into account the experimental errors in the laser energy control and the step used in the irradiation energy density we state a threshold of 0.92±0.03 for the ($A+B$)-to-B—type transition. The first detectable change by RBS of the nickel signal width is observed at 1.15 J/cm^2. Above this value mixing starts at the interface, thus indicating the melting of the underlying silicon. The energy width of the Ni signal increases almost linearly with increasing energy density of the laser pulse. The two experimental straight lines in the width versus energy density plot cross at 1.1±0.02 J/cm^2 which has been assumed as the threshold for interface mixing.

In summary, we have measured a threshold for $NiSi_2$ surface melting at 0.37±0.02 J/cm^2, a threshold for the ($A+B$)-to-B—type transition at 0.92±0.03 J/cm^2 and a threshold for the silicide silicon mixing at 1.1±0.02 J/cm^2.

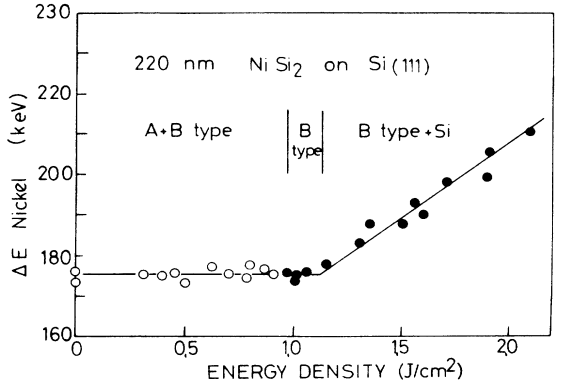

FIG. 4. Energy width of the Ni signal as obtained by 2.0 MeV He^+ RBS spectra against the laser pulse energy density. Open and closed circles refer to samples in which the silicide layer is $A+B$ type and B type, respectively. In the upper part the regions in which the irradiation results in a mixed $A+B$ $NiSi_2$ layer, in a B-type $NiSi_2$ layer and in a Si richer solution are denoted.

IV. DISCUSSION AND CONCLUSIONS

The observed silicide-silicon mixing indicates that melting of the underlying silicon occurs at 1.1 J/cm^2. It is then evident that the energy density required to melt the whole silicide layer is about 0.18 J/cm^2 lower than the one required to melt the silicon substrate. This fact excludes an interfacial melting such as that observed in the case of pure metal films on Si and suggests that a different melting temperature is associated with each side of the $NiSi_2$/Si interface.

To see if the observed melting dynamics can be explained on the basis of the Ni/Si phase diagram, let us first consider what would happen when a $NiSi_2$/Si system is heated up in thermodynamical equilibrium condition. In Fig. 5, the Ni/Si phase diagram is reported for Si concentration ranging between 50 and 100 at.% Si.[14] The $NiSi_2$ is a peritectic compound which at $T_P=1266$ K decomposes in liquid $Ni_{0.6}Si_{0.4}$ and in solid silicon, while

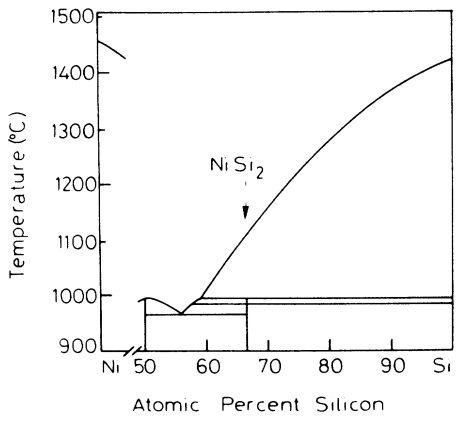

FIG. 5. Phase diagram of the Ni-Si system for Si concentration between 50 and 100 at. %.

the underlying silicon at the same temperature is in a stable phase. This decomposition should proceed via the $NiSi_2$ melting and solid silicon nucleation. With increasing temperature above T_P the Si content in the liquid increases and at the liquidus temperature $T_L = 1400$ K all the layer is liquid $NiSi_2$ on top of solid Si. At T_L there is equilibrium between the liquid $NiSi_2$ and the solid Si, i.e., the chemical potential of the Si atoms is the same in the solid Si and in the liquid $NiSi_2$. At temperatures above T_L the chemical potential of Si atoms is higher in solid Si than in liquid $NiSi_2$. To reach the equilibrium some silicon atoms must dissolve into the liquid solution. The silicon enrichment of the $NiSi_2$ layer is then expected at a temperature lower than the silicon melting point ($T_M = 1685$ K).

In the fast heating conditions provided by pulsed laser irradiation it is not known if the $NiSi_2$/Si system is allowed to follow the behavior described by equilibrium thermodynamics. We must then compare the duration of the heating induced by the laser pulse with the time required for the occurrence of each phase transformation predicted by the phase diagram.

A. $NiSi_2$/Si interface mixing

At temperatures higher than the liquidus temperature solid silicon dissolution in the molten $NiSi_2$ is expected. To estimate if the process kinetics is fast enough to occur during pulsed laser irradiation we can use a simple model where the solid Si dissolution velocity is expressed by[15]

$$v = \lambda \nu f e^{-E/k_B T}(1 - e^{-\Delta\mu/k_B T}), \quad (1)$$

where v is the liquid $NiSi_2$/solid-Si interface velocity, f is a site fraction [$f \sim 1$ (Ref. 16)], λ is an average jump distance (of the order of the solid-liquid interface thickness, ~ 3 Å), ν is an attempt frequency in the solid ($\sim 10^{13}$ sec^{-1}), E is the activation energy [0.7 eV/atom (Ref. 16)], T_i is the interface temperature and $\Delta\mu$ is the chemical potential difference of the Si atoms in pure Si and in the liquid solution at T_i. $\Delta\mu$ is a function of both temperature and Si concentration in the liquid solution.

$\Delta\mu$ can be obtained at any temperature from the free energy curves of both solid Si and liquid Ni-Si solution as a function of the silicon concentration. To calculate the free energy curve for the liquid we use the regular solution model.[17] The enthalpy interaction term is $H = X_{Ni} X_{Si}(\beta_1 X_{Ni} + \beta_2 X_{Si})$, where X_{Ni} and X_{Si} are the fractions of Ni and Si, respectively, and β_1 and β_2 are parameters which account for the interaction between the two different atoms in the solution. Standard free-energy values were used for liquid Ni and for solid and liquid silicon.[18] We estimated $\beta_1 = -64$ and $\beta_2 = -28$ Kcal/g atom by fitting the Ni/Si phase-diagram portion for temperature between 1250 and 1700 K and Si concentration between 60 and 100 at.%. A more sophisticated phase-diagram simulation of the Ni-Si system over the complete silicon concentration range has been performed by Kaufman.[19] In this computation the free energy of the liquid solution has been obtained taking into account both the enthalpy and entropy excess functions. Since this simulated phase diagram does not fit well the experimental one for Si concentration close to 0.67 in the high-temperature range, we performed, using the same model, a better fit in the concentration range actually investigated.

The chemical potential difference between silicon atoms in solid silicon and in liquid $NiSi_2$ at $T_i = T_L + 10$ K is of the order of 1 Kcal/g atom. Using this value the calculated solid silicon dissolution velocity in liquid $NiSi_2$ is 3 m/sec. The same calculation performed for the liquid-solid interface velocity of pure silicon at an interface temperature 10 K higher than the silicon melting temperature gives a value of 0.7 m/sec in agreement with the measured undercooling-interface velocity relationship of 17 K/m sec^{-1}.[16]

Despite the low $NiSi_2$ liquidus temperature respect to the Si melting temperature, the silicon atoms mobility at the interface, due to the chemical potential difference, is sufficiently high to produce silicon dissolution in the liquid $NiSi_2$ solution in a time interval as short as the duration of the laser-pulse-induced heating. In fact we have observed $NiSi_2$/Si interface shift of the order of tens of nanometer for melt duration of the order of hundreds of nanoseconds. The parameters in Eq. (1) are at all not well known but the order of magnitude of the calculated interface velocity should be correct. In fact the term $\lambda\nu$ must be of the order of the sound velocity and the activation energy was obtained[16] from a fit of the measured undercooling-interface velocity relationship in laser induced melting of pure Si. In Ref. 16 it was pointed out also that for small deviations from the equilibrium temperature overheating and undercooling effects on interface velocity are equal.

B. $NiSi_2$ surface melting

The other phase transformation prescribed by the phase diagram is the $NiSi_2$ decomposition at the peritectic temperature T_P. In fast heating condition nucleation processes are inhibited due to the low atomic mobility, and one would expect the $NiSi_2$ surface to melt at the metastable melting temperature T_0 at which the free energies of liquid and solid are identical, or the formation of superheated solid $NiSi_2$ up to the liquidus temperature. In this last case the two sides of the silicide-silicon interface should melt at the same temperature T_L, and this is in contrast with our experimental result in which the ($A+B$)-to-B—type transition (i.e., the melting of the whole silicide layer) occurs at an energy density about 0.18 J/cm^2 below silicon substrate melting.

Using for the calculation of liquid- and solid-$NiSi_2$ free energies the regular solution model previously described, and standard thermodynamical parameters,[20] respectively, we estimated T_0 to be about 10 K higher than the peritectic temperature. The slight difference between T_0 and T_P agrees with Kaufman's calculations,[19] where T_0 and T_P coincide.

Combining the experimental observations with the thermodynamic estimations the pulsed laser-induced dynamics of $NiSi_2$ on Si yields the following. At 0.37 ± 0.02 J/cm^2 the surface melts at $T_0 = 1276$ K, the melt depth increases with increasing the energy density of the laser pulse and reaches the silicide/silicon interface at

0.92 ± 0.03 J/cm^2, the underlying silicon melts at 1.1 ± 0.02 J/cm^2 when the silicide/silicon interface reaches $T_L = 1400$ K.

To test quantitatively the proposed mechanism and to correlate the maximum interface temperature with the energy density of the laser pulse we performed heat-flow calculations using the thermal model.[12] Standard thermal and optical parameters were used for the Si substrate.[22] A melting temperature of 1276 K was assumed for the $NiSi_2$ layer. The following parameters were used for the $NiSi_2$: solid reflectivity $R_S = 54\%$,[23] liquid reflectivity $R_L = 63\%$, solid absorption coefficient $\alpha_S = 10^5$ cm^{-1}, liquid absorption coefficient $\alpha_L = 8\times10^5$, solid thermal conductivity $K_S = 0.025$ cal/cm K sec at 313 K,[19] liquid thermal conductivity $K_L = 0.095$ cal/cm K sec, specific heat $c_p = 6$ cal/g atom, latent heat $C_1 = 9$ Kcal/g atom.

R_S and R_L are measured values using the Nd laser at 10° incidence angle, the solid reflectivity value agrees with the reported value.[23] The solid absorption coefficient has been estimated using the measured free carrier concentration[19] in $NiSi_2$ and assuming an absorption cross section $\sigma = 5\times10^{-18}$ cm^2.[24] However the value for α_S does not drastically affect the calculations because the heat profile is primarily controlled by thermal diffusion in the present case. A metallic absorption coefficient was used for the liquid and this value does not affect at all the calculation results. The solid thermal conductivity as a function of the temperature was obtained by interpolating data from Ref. 19. The liquid thermal conductivity is a weighted average of the liquid Ni and Si conductivity. Due to lack of existing data the specific heat was calculated using the Dulong and Petit rule. The calculated difference in the enthalpy contents of liquid and solid $NiSi_2$ at $T_0 = 1276$ K was used as a latent heat.

The surface melt duration obtained from heat flow calculations is reported as a continuous line in Fig. 2. The significant part of the curve is for energy densities below 1.1 J/cm^2, because at higher energy densities the calculation does not take into account the silicide-silicon mixing. The good agreement of the computed curve with the experimental data gives confidence to the proposed model and to the adopted parameters. In Fig. 6 the melt depth against the energy density of the laser pulse is reported. The surface melt threshold is 0.35 J/cm^2 and the melt front reaches the Si interface at 0.90 J/cm^2 in agreement with our observations within experimental uncertainty. At higher energy densities the interface temperature rises and reaches the $NiSi_2$ liquidus temperature at 1.04 J/cm^2 while the silicon melting point is reached at 1.21 J/cm^2 as indicated by the arrows in the diagram. The calculated energy density at which the interface reaches the Si melting point is higher than the one at which Si dissolution in the silicide layer is actually observed. The silicide-silicon mixing occurs instead at an energy density for which the calculated interface temperature is slightly higher than T_L.

The calculated energy density required to increase the interface temperature from T_0 to T_M or from T_0 to T_L are 0.31 and 0.14 J/cm^2, respectively. Those values depend mainly on the reflectivity and specific heat of the liquid solution. Both parameters are known with a good

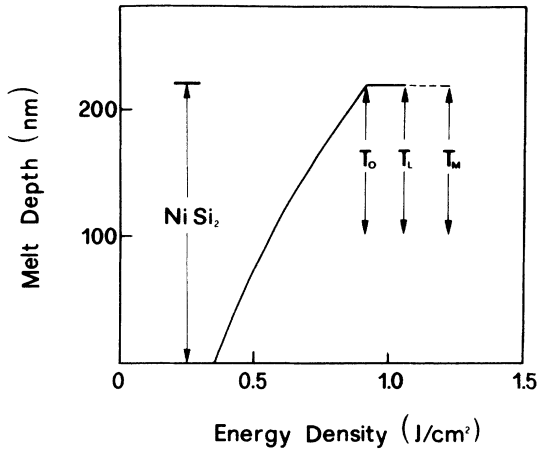

FIG. 6. Calculated melt depth as a function of the laser pulse energy density for the $NiSi_2$/Si system. The arrows indicate the energy densities at which the $NiSi_2$/Si interface reaches the $NiSi_2$ melting temperature (T_0), the $NiSi_2$ liquidus temperature (T_L) and the Si melting temperature (T_M). In the calculations a melting temperature of 1276 K (T_0) was assumed for the $NiSi_2$ layer.

accuracy; in fact the former has been measured and the latter cannot be markedly different from the one calculated using the Dulong and Petit rule. The 0.31 J/cm^2 energy density range seems overly large compared with the experimental one of 0.18 ± 0.05 J/cm^2 between the melting of the whole silicide layer and the mixing of Si. If the mixing occurs when the interface reaches the silicon melting point we must assume a specific heat of 4 cal/g atom for the liquid solution. This value is not a realistic one, so the calculations support the idea that silicon atoms dissolve into the liquid solution at $T = T_L$. However it must be pointed out that heat flow calculations can fit also the experimental data assuming T_L as the $NiSi_2$ melting temperature and T_M as the Si melting temperature at the interface. In any case surface melting and interfacial mixing occur at T_0 and T_L or T_L and T_M, respectively. Surface melting at T_0 and interfacial mixing at T_M is excluded by comparison of heat flow calculations with experimental data.

Our study of pulsed-laser-induced melting dynamics of a $NiSi_2$ layer on silicon have shown that melting starts at the $NiSi_2$ surface and proceeds toward the silicide-silicon interface. The melt depth increases with increasing the energy density until it reaches the interface. Solidification of such a layer results in a mainly B-type $NiSi_2$ crystal. Further increase of the energy density does not produce a thicker molten layer but only an increase of the interface temperature, melting of the underlying silicon occurs at a temperature higher than the $NiSi_2$ melting temperature so that interfacial melting at the eutectic temperature as observed in the case of a pure-metal film on top of silicon is excluded.[10,11]

Kinetics and thermodynamical considerations give

plausibility to the statement that $NiSi_2$ melts at a metastable temperature T_0 very close to its peritectic temperature and that the Si at the interface dissolves into the molten $NiSi_2$ at the liquidus temperature as predicted by the phase diagram. These two temperatures allow a good fit of the experimental data with heat flow computations. In the alternative hypotesis of Si melting at T_M we were not able to get a satisfactory fit of the experimental data unless we assumed the existence of a superheated solid $NiSi_2$ up to the $NiSi_2$ liquidus temperature T_L.

ACKNOWLEDGMENTS

We are grateful to S. U. Campisano for his many fruitful comments and to N. Marino for technical assistance with the Nd glass laser.

[1]M. O. Thompson, J. W. Mayer, A. G. Cullis, M. C. Webber, N. G. Chew, J. M. Poate, and P. C. Jacobson, Phys. Rev. Lett. **50**, 896 (1983).

[2]P. Baeri, G. Foti, J. M. Poate, and A. G. Cullis, Phys. Rev. Lett. **45**, 2036 (1980).

[3]A. G. Cullis, M. C. Webber, N. G. Chew, J. M. Poate, and P. Baeri, Phys. Rev. Lett. **49**, 219 (1982).

[4]K. A. Jackson, in *Surface Modification and Alloying,* edited by J. M. Poate, G. Foti, and D. C. Jacobson (Plenum, New York, 1983), Chap. 3.

[5]C. W. White, D. M. Zehner, S. U. Campisano, and A. G. Cullis, in *Surface Modification and Alloying,* Ref. 4, Chap. 4.

[6]M. Von Allmen and S. S. Lau, in *Laser Annealing of Semiconductors,* edited by J. M. Poate and J. W. Mayer (Academic, New York, 1982), p. 439.

[7]M. Von Allmen, S. S. Lau, T. T. Sheng, and M. Wittmer, in *Laser and Electron Beam Processing of Materials,* edited by C. W. White and P. S. Peercy (Academic, New York, 1980), p. 524.

[8]G. Majni, F. Nava, G. Ottaviani, A. Luches, V. Nassisi, and G. Celotti, Vacuum **32**, 11 (1982).

[9]M. G. Grimaldi, P. Baeri, E. Rimini, and G. Celotti, Appl. Phys. Lett. **43**, 244 (1983).

[10]R. Fastow, J. W. Mayer, T. Brot, M. Eizemberg, and J. O. Olowolafe, Appl. Phys. Lett. **46**, 1052 (1985).

[11]P. Baeri, S. U. Campisano, F. Priolo, and E. Rimini, in *Energy Beam Solid Interactions and Transient Thermal Processing,* Proceedings of the Material Research Society Meeting (Strasbourg), edited by V. T. Nguyen and A. G. Cullis (les éditions de Physique, les Ulis, 1985), p. 237.

[12]R. T. Tung, J. M. Gibson, and J. M. Poate, Phys. Rev. Lett. **50**, 429 (1983).

[13]R. T. Tung, J. M. Gibson, D. C. Jacobson, and J. M. Poate, Appl. Phys. Lett. **43**, 476 (1983).

[14]M. Hansen, *Constitution of Binary Alloy* (McGraw-Hill, New York, 1958), p. 1040.

[15]D. Turnbull and M. H. Cohen, in *Modern Aspects of the Vitreous State,* edited by J. D. Mackenzie (Butterworth, London, 1960), p. 38.

[16]M. O. Thompson, P. H. Bucksbaum, and J. Bokor, in *Energy Beam Solid Interaction and Transient Thermal Processing,* Proceedings of the Material Research Society Meeting (Boston), edited by D. K. Biegelsen, G. A. Rozgony, and C. V. Shank (Materials Research Society, Pittsburgh, 1984), p. 181.

[17]P. Haasen, *Physical Metallurgy* (Cambridge University Press, Cambridge, 1978), p. 81.

[18]R. Hultgreen, P. D. Desai, D. T. Hawkins, M. Gleiser, K. K. Kelley, and D. D. Wagman, *Selected Values of the Thermodynamic Properties of the Elements* (American Society for Metals, Cleveland, 1973).

[19]L. Kaufman, Comput. Coupling Phase Diagrams & Thermochem. **3**, 45 (1979).

[20]M. A. Nicolet and S. S. Lau, in *VLSI Electronics: Microstructure Science* (Academic, New York, 1983), Vol. 6, Chap. 6.

[21]P. Baeri and S. U. Campisano, *Laser Annealing of Semiconductors,* Ref. 6, Chap. 4.

[22]A. Goldsmith, T. Waterman, and H. Hirschhorn, *Handbook of Thermophysical Properties of Solid Materials* (Macmillan, New York, 1961), Vol. I.

[23]A. Humbert and A. Cross, J. Phys. (Paris) Lett. **44**, 929 (1983).

[24]K. G. Svantesson, J. Phys. D **12**, 425 (1979).